PHYSICAL REVIEW B VOLUME 34, NUMBER 4 15 AUGUST 1986

Photoconductivity and light-induced change in a-Si:H

T. J. McMahon and J. P. Xi*
Solar Energy Research Institute, Golden, Colorado 80401
(Received 3 February 1986)

Capture-rate constants for the trapping of free carriers into different gap-state species are determined by calculating dc photoconductivity at intermediate generation rates versus the inverse temperature and fitting to data measured on undoped a-Si:H in the as-grown and light-soaked states. In the as-grown state, recombination is dominated by high-capture-rate centers near the Fermi level (dangling bonds) at and above 300 K. To explain the second peak and rapid decrease in photoconductivity at lower temperatures, an energy-dependent capture rate must be invoked on the smaller-cross-section band-tail states, indicating a multiphonon energy-loss process for the trapping of free charge. After 90 h of exposure to 100 mW/cm^2 of light, the decrease found in photoconductivity is explained only by increases in both dangling-bond recombination at and above room temperature *and* tail-state recombination at lower temperatures. The increased recombination at lower temperatures after light soaking is attributed to additional donor states located 0.23 eV above the valence-band edge.

I. INTRODUCTION

Very few characterization procedures are sensitive to the gap-state distribution $g(E)$ and capture-rate constant $K(E)$ over very much of the energy gap in a-Si:H. To facilitate the methods that are [e.g., isothermal capacitance-transient spectroscopy[1] (ICTS) and deep-level transient spectroscopy[2] (DLTS)], doping of the intrinsic material (usually with P) is required to increase its conductivity. On the other hand, dc photoconductivity, σ_{pc}, versus temperature, T, can be carried out with relative ease on intrinsic as well as doped a-Si:H, probing recombination through most of the energy gap. Shockley-Read-Hall recombination statistics[3] can be used to model dc photoconductivity with a modified Simmons and Taylor[4] calculation. At the outset we wish to point out that, while temperature dependent σ_{pc} has been used extensively to characterize a-Si:H and calculations have been carried out at a single temperature or over a restricted range to study the photon-flux power-law dependence and to determine the capture rate of a single trap species,[5,6] this is the first calculation that fits values of σ_{pc} versus $10^3/T$ to measured data over so large a temperature range. Such fitting is a most useful probe for the understanding of the gap-state trapping and recombination properties of a-Si:H and changes in them caused by light-induced degradation. We use a simple density-of-states distribution, $g(E)$, composed of 10^{16} cm^{-3} dangling bonds and exponential tail states, to calculate values of σ_{pc} for a-Si:H in the as-grown (AG) state. Because fitting to experimental values is carried out for temperatures between 120 and 400 K at three generation rates (each separated by a factor of 10), trap quasi-Fermi-levels have moved far enough through the gap that capture rate and adjustment of $g(E)$ can be determined for nearly the entire gap. This multiple-trap-species approach is required to explain properly σ_{pc} over the entire temperature range and avoids errors in power-law—dependence arguments based on single-trap-species calculations, especially at room temperature, where electronic doping is quite evident. Our cross section values are much smaller than those found by Street.[7]

After a baseline is established for $g(E)$ and $K(E)$ for dangling bonds and tail states in the AG state, the film is exposed to 100 mW/cm^2 for 90 h with the temperature kept below 35 °C to achieve the light-soaked (LS) state. The altered $g(E)$ includes an additional 1.5×10^{16} cm^{-3} dangling bonds to explain the decrease in σ_{pc} at and above room temperature. Researchers have known about the creation of these additional spins for some time,[8] as well as their effect on σ_{pc}.[9,10] In addition, however, we find the large decrease in σ_{pc} at lower temperatures to be the result of recombination at 1.5×10^{18} cm^{-3}, light-induced donors (LID's) located 0.23 eV above the valence-band edge (E_v). Approximately this many LID's were first measured by DLTS, but were located 0.35 eV above E_v.[2] Vanier has suggested that such LID's could explain the large decreases in σ_{pc} that he observed at lower temperatures.[11] The fact that we find these states located nearer to E_v than found by Lang *et al.*[2] may explain why they have never been observed as a change in Urbach-tail width.[12,13] Though we do find an increase in the dark-conductivity activation energy from 0.70 to 0.77 eV, we make no attempt to account for this by the introduction of light-induced acceptors.

With light soaking we also observed the increase in sub-band-gap σ_{pc},[14] and hence absorption as found by Han and Fritzsche,[15] and we suggest that these are the dangling-bond states which will also reduce σ_{pc} for above-band-gap photons. The effect of electronic doping,[16] which manifests itself as infrared quenching[17] and as the lower-temperature peak in σ_{pc} versus T,[14] does indeed diminish with the production of LID's, masking the effect of the lower-capture-rate, deep tail states (agreeing with the conclusions of Han and Fritzsche[15]). We find that the capture rates for the dangling bonds and the LID's are both very large compared to the low-capture-

 ©1986 The American Physical Society

rate centers, which are due to the unaffected deep-tail states.

After a vacuum anneal at 160 °C for 2 h, the annealed (AN) state is achieved, and values of σ_{pc} show only a partial recovery. Curve fitting required that the dangling bonds be restored to their AG values, but some LID's must remain. On the other hand, the dark conductivity returned to the AG values, with an activation energy of 0.70 eV.

II. SAMPLE PREPARATION AND EXPERIMENTAL DETAILS

The films were prepared by the rf glow-discharge technique at 250 °C using pure SiH_4 at a deposition rate of 2 Å/sec. The 5000-Å-thick intrinsic layer was deposited on Corning 7059 glass for σ_{pc} and dark-conductivity characterization. A bias of 20 V was applied across two 10-mm-long silver epoxy contacts spaced 1 mm apart in the gap-cell configuration. Though only one film was fully characterized with matching calculations in this study, we checked several films made at our laboratory and found their behavior to be typical of the film under study. We also note that such general features in the σ_{pc}-versus-$(1/T)$ data taken both after light soaking and after annealing have also been found at three other laboratories (see Refs. 10, 11, and 15) and conclude that the calculations and results found in this study would apply to most intrinsic *a*-Si:H films.

During σ_{pc} characterization, data were taken with white light from an a tungsten lamp filtered to pass only 630 nm to produce as uniform a generation rate as possible while maintaining an adequate generation rate G. In the calculation and curve fitting, uniform values of G are calculated with the following equation:

$$G(630\ \text{nm}) = (1 - e^{-\alpha(630\ \text{nm})d}) N_{ph}/d \ , \tag{1}$$

where d in cm is the film thickness, $\alpha(630\ \text{nm})$ is the absorption coefficient at 630 nm in cm^{-1}, and N_{ph} is the photon density in photons/cm^2 sec. The photocurrent is the total current minus the dark current. Neutral density filters were inserted to take data for lower values of G. The light soaking was carried out in air with unfiltered ELH light at a level of 100 mW/cm^2 and at a temperature maintained below 35 °C. Annealing was done in vacuum at 160 °C for 2 h.

III. PHOTOCONDUCTIVITY

A rigorous solution to the nonequilibrium, steady-state recombination equations for materials with continuous distributions of traps[4] allows σ_{pc} versus $10^3/T$ to be calculated [shown as lines in Figs. 1(a)–1(c)] and therefore provides a way to determine $g(E)$ and $K(E)$ for AG, LS, and AN states. We use

$$\sigma_{pc} = (n - n_0)e\mu_n + (p - p_0)e\mu_p \ , \tag{2}$$

where μ_n, the extended-state mobility for the free electrons n, is taken to be 13 cm^2/V sec,[18] and μ_p, the extended-state mobility for free holes p, is 1 cm^2/V sec. Dark free-electron and -hole concentrations are given by n_0 and p_0, respectively. In steady state, G is equal to the recombination minus the thermal emission as expressed by

$$G = \sum_i \int_{E_v}^{E_c} \{ nK_n^i(E)[1 - f_i(E)] - e_n^i f_i(E) \} N_i(E) dE \ , \tag{3}$$

where $N_i(E)$ is the number of traps of the ith species at energy E, as measured upward from the valence-band edge E_v, to the conduction-band edge E_c. $K_n^i(E)$ is the energy-dependent capture rate for electrons to $N_i(E)$ and $e_n^i(E)$ is the thermal-emission term,

$$e_n^i(E) = K_n^i(E) N_c \exp\left[\frac{E - E_c}{kT}\right] , \tag{4}$$

and $f_i(E)$, the trap-occupancy function for the ith species, is given by

$$f_i(E) = \frac{nK_n^i(E) + e_p^i(E)}{nK_n^i(E) + pK_p^i(E) + e_n^i(E) + e_p^i(E)} \ , \tag{5}$$

where p subscripts correspond to hole terms. N_c is the effective density of states at the band edge. Equation (3) and the charge-neutrality condition

$$p - n = \sum_i \int_{E_v}^{E_c} N_i^a(E) f_i(E) dE - \sum_j \int_{E_v}^{E_c} N_j^d(E)[1 - f_j(E)] dE \tag{6}$$

are solved numerically for n and p over the range of T and G of interest. A discussion of the results follows.

In the *AG state*, two species of $N_i(E)$ composing $g(E)$ were used: The first, dangling-bond states, D_3^0, are shown in Fig. 2(a) as two Gaussians split by an energy 0.5 eV centered at about $E_F = 1.1$ eV with peak values of 5×10^{16} $\text{cm}^{-3}\,\text{eV}^{-1}$. The lower peak corresponds to the energy distribution of neutral, singly occupied dangling bonds having an integrated value of $N_s = 1.1\times10^{16}$ cm^{-3}. Though a spin-density measurement has not been made, this value was used because it corresponds to material at the lower end of spin-density determinations (see Refs. 7 and 10 for values of 5×10^{15} cm^{-3} and Ref. 19 for 10^{16} cm^{-3}). The widths and splitting have been determined through trial-and-error curve fitting. The splitting of 0.5 eV corresponds to the correlation energy required to add a second electron to a singly occupied dangling bond. This is not to be confused with the energy difference between trapped electrons and holes in D_3^0 states. We treat these as being donorlike [labeled $D_3^d(E)$] with a capture-rate constant $K_p^{D_3^d}$ corresponding to the trapping of a free hole at an occupied D_3^d state [see Eq. (7) and process (4) in Fig. 3(a)]. The upper peak corresponds to doubly occupied, negatively charged dangling bonds, which are labeled $D_3^a(E)$. These are unoccupied for intrinsic *a*-Si:H when $G = 0$. In the empty state they are treated as acceptors having a neutral capture-rate constant for electrons designated as $K_n^{D_3^a}$ in Eq. (8) and shown as process (1) in Fig. 3(a). Equations (7) and (8) are shown to describe these recombination processes only when the traps are between

the trap quasi-Fermi-levels, E_{Fn}^{t} and E_{Fp}^{t}, for electrons and holes, respectively. Though these equations are never explicitly used, the transition rates represented are implicitly accounted for in solving Eqs. (3) and (6),

$$\frac{dp}{dt}=\int_{E_v}^{E_c}[pK_p^{D_3^a}f_D(E)D_3^a(E)+pK_p^{D_3^d}f_D(E)D_3^d(E)]dE\ , \tag{7}$$

$$\frac{dn}{dt}=\int_{E_v}^{E_c}\{nK_n^{D_3^a}[1-f_D(E)]D_3^a(E)+nK_n^{D_3^d}[1-f_D(E)]D_3^d(E)\}dE\ . \tag{8}$$

Figure 3(a) also shows the recombination processes at dangling bonds. Process (3) involves the recombination of a free hole with a trapped electron, n_t, but only when the state lies below E_{Fn}^{t} and is less likely to emit back to the conduction-band edge E_c. The rate constant of this free hole recombining with n_t is designated $K_p^{D_3^a}$ in Eq. (7). The corresponding recombination-rate constant of a free electron with a trapped hole is designated as $K_n^{D_3^d}$ in Eq. (8) and shown as process (2) in Fig. 3(a).

Clearly, whether or not a defect with a trapped charge acts as a recombination center depends on the level of G and the temperature T. Higher G increases n and p, making recombination more likely and resulting in greater

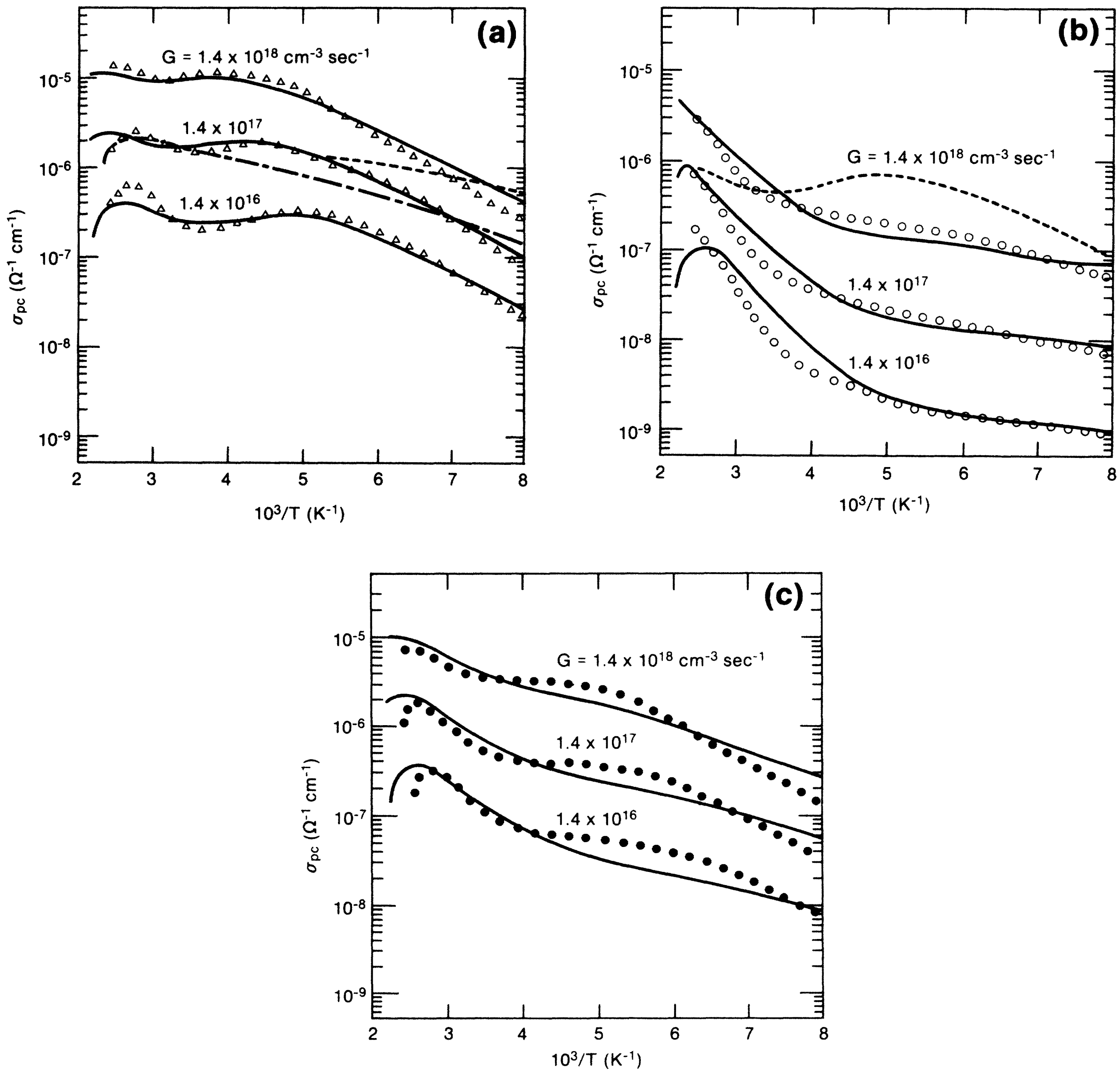

FIG. 1. Photoconductivity vs $10^3/T$ data (points) and calculated values (lines) at values of G as shown. (a) AG state with charged-to-neutral capture-rate constant ratios of 1 (——) and 1000 (—-—-), or with a constant capture rate for tail states (— — —); (b) LS state with (——) and without (— — —) LID's; and (c) AN state.

trap quasi-Fermi-level splitting. Reducing T lowers the emission probability of the trapped charge, leading to increased recombination at shallower states and, as before, a greater trap quasi-Fermi-level splitting. Over the temperature range used here, the quasi-Fermi-level splitting ranges between 0.25 and 1.4 eV, allowing for the different trap species to be fitted relatively independently of each other. We note that the recombination process is usually limited by the free carrier to neutral-center capture-rate constants $K_n^{D_3^a}$ and $K_p^{D_3^d}$; this is reasonable as there is no added Coulombic attraction. Therefore, most traps would not contain trapped charge if $n=p$ and the gap-state distribution is symmetrical. In intrinsic a-Si:H, however, the valence-band tail is much broader than the conduction-band tail, and n is at least 10 times p, with the result that the $D_3^a(E)$ state is highly occupied for nontrivial values of G.

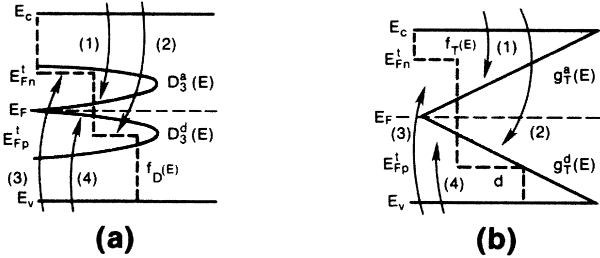

FIG. 3. Illustration of the occupancy functions with trapping and recombination processes at (a) dangling bonds and (b) tail states. These four processes are described in the text.

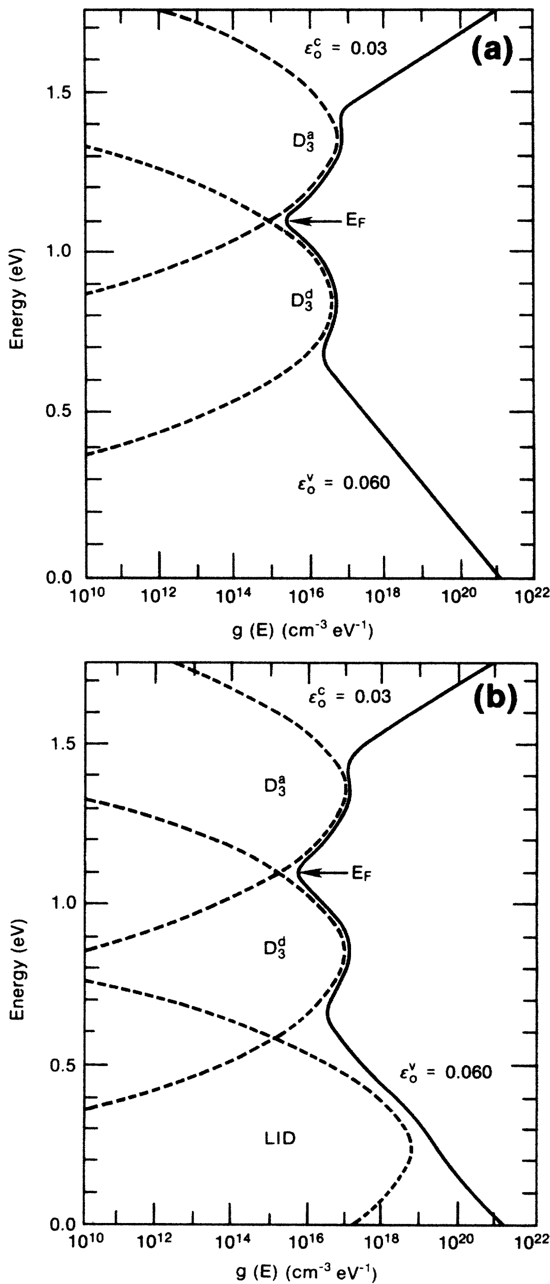

FIG. 2. Total density of states (——) with dangling bonds for (a) the AG state and with additional dangling bonds and LID's for (b) the LS state.

Since it has been suggested, by Hack and Shur[6] for phosphorus-doped a-Si:H, that the ratio of charged to neutral capture-rate constants may be as high as 1000, we decreased the neutral capture-rate values by a factor of 10^{-3} for each of the donorlike and acceptorlike dangling-bond and tail states with separate distribution functions to obtain the dashed-dotted line in Fig. 1(a) for the intermediate value of G. Since the calculated values are not too different, but the structure due to electronic doping is nearly absent as a result of the large capture-rate differential, we choose to equate the charged and neutral capture-rate constants, $K_p^{D_3^a}=K_p^{D_3^d}$, etc., as do Simmons and Taylor.[4] This reduces the number of free parameters and allows the use of only one trap Fermi function for dangling bonds, $f_D(E)$, or tail states, $f_T(E)$. The curve-fitting procedure is greatly simplified, and for curve fitting at room temperature and above, capture-rate values of $K_n^{D_3^a}=1\times10^{-9}$ cm^3 sec^{-1} and $K_p^{D_3^d}=1\times10^{-10}$ cm^3 sec^{-1} are obtained. Fitting for the latter value is not very sensitive and was arrived at as an approximate ratio of the free-carrier mobilities. Table I summarizes the constants and parameters used in all the fitting to clarify what is assumed and what is determined through fitting to experimental data.

The former value may be compared to the capture cross section for the trapping of an electron at a singly occupied dangling bond of 3.4×10^{-15} cm^2 measured by Street.[7] If a thermal velocity can be used for the conversion, then we have measured a much smaller value of 10^{-16} cm^2. We note in passing that such a value does not convert directly into the physical size of the trap, since a factor for energy loss is also implicit in the transition probability to the bound state. Street's result, which is 34 times larger, could be the result of neglecting trapped charge in spinless tail states, which will be significant for his range limited determinations. The furthest the demarcation energies

move from their respective mobility edges is 0.34 eV for the longest time considered (10^{-6} sec). The fact that his values of $\mu\tau_D$ still decrease with increasing spin density is presumably due to the fact that spinless tail-state defects are also increasing in number.[20] In our measure, the effects of dangling-bond and tail states are each determined. If we had chosen the smaller spin value, $N_s=5\times10^{15}$ cm^{-3}, the best-fit capture-rate values would have been 10 times larger. However, the high-T peak is lowered by 30% while retaining the fit for the lower-T peak. For this reason and for reasons to be discussed for the light-induced dangling bonds, we believe the smaller capture values acquired using $N_s=1.1\times10^{16}$ cm^{-3} are more appropriate and note that they are only a factor of five smaller than those obtained by Hack *et al.*[6]

The second species of states for the AG film are donorlike and acceptorlike tail states exponentially decreasing in density from E_v and E_c with characteristic energies of $\varepsilon_0^v=0.060$ eV and $\varepsilon_0^c=0.030$ eV, respectively, as shown in Fig. 2(a). The corresponding trapping and recombination processes are shown in Fig. 3(b). If no energy dependence is used for the capture-rate constants of the band-tail states, the best fit to the low-temperature σ_{pc} data for the AG state that can be obtained is shown by the shallow dashed curve for the intermediate value of G in Fig. 1(a). In order to match the steeper slope, the capture-rate constants $K_n^T(E)$ and $K_p^T(E)$ must increase rapidly as the trap quasi-Fermi-levels approach their respective band edges. For tail states 0.15 eV and further from the mobility edges, the calculated solid line matches the data at all T if we share the energy dependence equally, using

$$K_p^T(E)=2\times10^{-7}\exp[(E_v-E)/(0.027\text{ eV})]\text{ cm}^3\text{sec}^{-1} \quad (9)$$

and

$$K_n^T(E)=2\times10^{-7}\exp[(E-E_c)/(0.027\text{ eV})]\text{ cm}^3\text{sec}^{-1}\ . \quad (10)$$

Physically, we expect such a dependence to result from a multiphonon, energy-loss process[21] and note that such an exponential dependence has once before been observed in the conduction-band tail region of a-Si:H using ICTS,[1]

TABLE I. Constants and parameters.

Symbol	Value	Comment
E_F	1.1 eV	dark conductivity
μ_n	13 cm^2/V sec	Ref. 18
μ_e	1 cm^2/V sec	Assumed—not critical
	$D_3^d(E)$, $D_3^a(E)$ states	
N_s	1.1×10^{16} cm^{-3}	Ref. 19
Location	0.85 eV, 1.35 eV	Gaussians symmetrically placed about E_F
Correlation energy	+0.5 eV	from best fit
Width	as shown	from best fit
$K_n^{D_3^a}$	10^{-9} cm^{3}sec^{-1}	form best fit
$K_p^{D_3^d}$	10^{-10} cm^{3}sec^{-1}	Assumed to be $\frac{1}{10}K_n^{D_3^a}$
	$g_T^d(E)$, $g_T^a(E)$ states	
$g_T^d(E_v)$, $g_T^a(E_c)$	10^{21} cm^{-3}eV^{-1}	assumed from crystalline Si
ϵ_0^v	0.060 eV	exponential dependence from Ref. 18 but with slope decreased to match the Urbach absorption edge
ϵ_v^c	0.030 eV	
$K_p^T(E)$ and $K_n^T(E)$	See text above	
	Light-induced states	
$K_n^{D_3^a}$	10^{-9} cm^{3}sec^{-1}	assumed to be the same as intrinsic D_3^0 capture rates
$K_p^{D_3^d}$	10^{-10} cm^{3}sec^{-1}	
N_s'	1.5×10^{16}	from best fit
No. of LID's	1.1×10^{18} cm^{-3}	Ref. 2
Location	0.23 eV	Gaussian located from best fit
Width	as shown	from best fit
K_n^{LID}	3×10^{-9} cm^{3}sec^{-1}	from best fit

but was associated with a bump in the density of states at $E_c - E = 0.50$ eV. A direct comparison to those results is not appropriate, since we associate the exponential capture-rate constant to band-tail states. It should be noted that the characteristic energy of 0.027 eV is between the zone-boundary acoustic- and optic-phonon energies of crystalline silicon. Now the capture rate for holes (electrons) in shallow neutral donor (acceptor) band-tail traps populate at an exponentially increasing rate as trap levels are closer to E_v (E_c). The subsequent recombination rate for electrons (holes) is proportionally increased through detailed balance as the trap quasi-Fermi-level moves through these shallower traps. On the other hand, deeper tail states have a smaller capture-rate constant than the neighboring D_3^0 states, resulting in the observed low-T peak due to electronic doping[16] at $10^3/T \approx 3.5-5$ K^{-1}.

The reason for this peak in photosensitivity is evident in the AG values of trapped-hole populations shown in Fig. 4. As the trap quasi-Fermi-levels move through the high-capture-rate dangling bonds into the neighboring tail states with the lowering of T, the trapped holes in dangling bonds begin to depopulate while the lower-capture-rate tail states populate. For this limited temperature range electronic doping occurs. σ_{pc} increases and then again falls as the shallower tail states become recombination centers with further reduction of T. Curve fitting at lower T was started with band-tail characteristic energies determined from time of flight[18] and needed to be increased to the values noted above for better fits. A trade-off *cannot* be made between band-tail slope and capture-rate energy dependence since a critical trapping balance must be maintained between D_3^d and deeper tail states. A value of 0.060 eV is also quite consistent with Urbach-tail measurements which occur over the same energy range.

In the *LS state* an additional 1.5×10^{16} states/cm^3 must be added to $g(E)$ as dangling bonds [see Fig. 2(b)] to calculate the decreases observed in the σ_{pc}-versus-($10^3/T$) data [Fig. 1(b)] at and above room temperature if the same capture rates as before are to be used. If we had chosen to use the larger capture-rate constant obtained for the smaller initial spin density, then only half as many light-induced spins would have been generated—not agreeing well with ESR results.[10,19] Figure 1(b) shows the effect of electronic doping being much smaller in the σ_{pc}-versus-($10^3/T$) curve. This implies that the capture rate for band-tail states below the D_3^d states must now be approximately the same as the dangling bonds with a much smaller energy dependence, as suggested earlier,[14] or a species of competing traps could be produced (as found by Lang *et al.*[2]) with a capture rate similar to the rate found for the dangling bonds. We prefer the latter choice as the more physical explanation, even though the former argument will have a similar overall effect on the recombination process, since (1) these donors have been observed by DLTS (Ref. 2) and the location in which we find them does not conflict with the results of absorption measurements,[12,13] and (2) a change in capture rate without a change in its gap-state energy would be highly coincidental. To achieve the fits shown in Fig. 1(b), we added approximately the same number of LID's as found by Lang *et al.*[2] near E_v and left the tail states unchanged. These donor states were distributed as follows:

$$g_{\rm LID}(E) = 5\times10^{18}\exp[-(E-0.23\ {\rm eV})^2/(0.015\ {\rm eV}^2)]\ , \tag{11}$$

which has an integrated value of 1.1×10^{18} states/cm^3 centered 0.23 eV above E_v. The capture-rate constant for these LID's is determined through curve fitting at lower T to be 3×10^{-9} cm^3 sec^{-1}. To demonstrate the important effect that these states have on the curve fits at low temperature, we show the calculation done without LID's for the intermediate value of G in Fig. 1(b) as the dashed line. Below room temperature the lower-capture-rate tail states have no competition from the high-capture-rate LID's, and the electronic doping effect is as evident in the σ_{pc} values as it is in the AG case, even though many more D_3^0 states are present. Such a placement of LID's is consistent with the enhanced field found near the p/i interface in solar cells after light soaking.[22]

For the *AN state*, Fig. 1(c) shows measured values of σ_{pc} which are still below those found for the AG state, though the dark conductivity and activation energy are entirely restored. To fit these data, the dangling bonds had to be restored to their original value, while the LID's could only be decreased to a value of 1×10^{17} cm^{-3} to obtain the best fit.

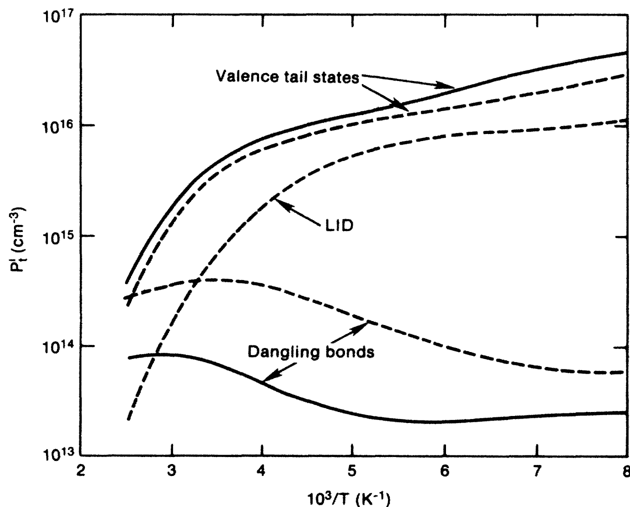

FIG. 4. Trapped-hole populations vs $10^3/T$ of (a) the AG state (——) and (b) the LS state (— — —).

IV. SUMMARY

For the first time, values for σ_{pc} versus $10^3/T$ at various generation rates have been calculated that match observed values on a-Si:H in the AG, LS, and AN states. To calculate the two-peaked behavior in measured σ_{pc}-versus-($10^3/T$) results on AG a-Si:H, a density-of-states spectrum $g(E)$ composed of dangling-bond states with a positive correlation energy must be used, along with an exponential tail-state distribution having an energy-dependent capture rate. The capture-rate constant for an

electron into a neutral dangling bond is found to be 10^{-9} $cm^3 sec^{-1}$, and if the charged-to-neutral capture-rate—constant ratio is greater than 1, this value represents the larger value. We suggest that the transition probability to these states is so small because the energy-loss process is similar to the one we find for tail states.

For a satisfactory fit at lower temperatures, the capture-rate dependence for the trapping of free carriers in the band-tail states must decrease rapidly as trapping occurs deeper in the gap. Such a dependence is indicative of a multiphonon energy-loss process.[21] It is also clear, after studying the family of curves shown in Fig. 1, that some of the conclusions drawn in the past from constant T plots of σ_{pc} versus G may need to be modified, i.e., the values of σ_{pc} and therefore the separation of curves at room temperature is apparently controlled by the interaction of two species of traps and physical insight drawn from one species treatments may be inappropriate.

In the LS state we see the effect of two kinds of defects: First, we find the decrease in σ_{pc} at and above room temperature to be the result of light-induced dangling bonds. These dangling bonds may well have the same capture-rate constants as found for intrinsic dangling bonds. Second, the loss in σ_{pc} below room temperature is attributed to LID's in the lower half of the mobility gap, as found by DLTS measurements.[2] However, we find them located only 0.23 eV above E_v instead of 0.35 eV above E_v, as found by Lang *et al.*[2] In this lower position they would not be observable as a change in the Urbach-tail width, which is indeed the case. Such LID's are also consistent with the steeper potential profile observed at the p/i interface in degraded p-i-n solar cells.[22] Finally, with 160 °C annealing we find that all of the light-induced dangling bonds disappear, while approximately 10% of the LID's remain.

ACKNOWLEDGMENTS

We wish to thank Dr. R. Könenkamp for technical discussions, Dr. S. K. Deb and Dr. R. Tsu for their support of this work, and Dr. S. Kurtz and Dr. J. Pankove for their critical reading of the manuscript. This work was funded by the U.S. Department of Energy under Contract No. DE-AC02-83CH10093.

---

*Also at: Department of Physics, Colorado School of Mines, Golden, CO 80401.

[1]H. Okushi, Y. Tokumaru, S. Yamasaki, H. Oheda, and K. Tanaka, Phys. Rev. B **27**, 5184 (1983).

[2]D. V. Lang, J. D. Cohen, J. P. Harbison, and A. M. Sergent, Appl. Phys. Lett. **40**, 474 (1982).

[3]W. Shockley and W. T. Read, Jr., Phys. Rev. **87**, 835 (1952).

[4]J. G. Simmons and G. W. Taylor, Phys. Rev. B **4**, 502 (1971).

[5]C. R. Wronski and R. E. Daniel, Phys. Rev. B **23**, 794 (1981).

[6]M. Hack, S. Guha, and M. Shur, Phys. Rev. B **30**, 6991 (1984).

[7]R. A. Street, Appl. Phys. Lett. **41**, 1060 (1982).

[8]H. Dersch, J. Stuke, and J. Beichler, Appl. Phys. Lett. **38**, 456 (1981).

[9]D. L. Staebler and C. R. Wronski, Appl. Phys. Lett. **31**, 292 (1977).

[10]H. Dersch, L Schweitzer, and J. Stuke, Phys. Rev. B **28**, 4678 (1983).

[11]P. E. Vanier, Appl. Phys. Lett. **41**, 986 (1982).

[12]A. Skumanich, N. M. Amer, and W. B. Jackson, Phys. Rev. B **31**, 2263 (1985).

[13]D. Han and H. Fritzsche, in *Optical Effects in Amorphous Semiconductors*, AIP Conf. Proc. No. 120, edited by P. C. Taylor and S. G. Bishop (AIP, New York, 1984), p. 296.

[14]T. J. McMahon and J. P. Xi, J. Non-Cryst. Solids **77&78**, 409 (1985).

[15]D Han and H. Fritzsche, J. Non-Cryst. Solids **59&60**, 397 (1983).

[16]A. Rose, *Concepts in Photoconductivity and Allied Problems* (Interscience, New York, 1963), pp. 48—53.

[17]P. E. Vanier and R. W. Griffith, J. Appl. Phys. **53**, 3098 (1982).

[18]T. Tiedje, J. M. Cebulka, D. L. Morel, and B. Abeles, Phys. Rev. Lett. **46**, 1425 (1981).

[19]M. Stutzmann, W. B. Jackson, and C. C. Tsai, Phys. Rev. B **32**, 23 (1985).

[20]W. B. Jackson and N. M. Amer, Phys. Rev. B **25**, 5559 (1982).

[21]C. H. Henry and D. V. Lang, Phys. Rev. B **15**, 989 (1977).

[22]D. E. Carlson, A. R. Moore, D. J. Szostak, B. Goldstein, R. W. Smith, P. J. Zanzucchi, and W. R. Frenchu, Solar Cells **9**, 19 (1983).